Appl. Math. Mech. -Engl. Ed., **38**(4), 469–478 (2017)
DOI 10.1007/s10483-017-2189-6

Applied Mathematics and Mechanics (English Edition)

Analytical study of wrinkling in thin-film-on-elastomer system with finite substrate thickness*

Xianhong MENG[1,†], Guanyu LIU[1], Zihao WANG[1], Shuodao WANG[2]

1. School of Aeronautic Science and Engineering, Beihang University, Beijing 100191, China;
2. School of Mechanical and Aerospace Engineering, Oklahoma State University, Stillwater, OK 74078, U. S. A.

Abstract Surface wrinkling, a film bonded on a pre-strained elastomeric substrate can form periodic wrinkling patterns, is a common phenomenon in daily life. In existing theoretical models, the film is much thinner than the substrate so that the substrate can be considered to be elastomeric with infinite thickness. In this paper, the effect of finite substrate thickness is analyzed theoretically for free boundary condition cases. Based on the minimum potential energy principle, a theoretical model is established, and the wave length and amplitude of the wrinkling pattern are obtained. When the thickness of the substrate is more than 200 times larger than the thickness of the film, the results of this study agree well with the results obtained from the previous models for infinite substrate thickness. However, for thin substrates, the effect of finite substrate thickness becomes significant. The model given in this paper accurately describes the effect of finite substrate thickness, providing important design guidelines for future thin-film-on-substrate systems such as stretchable electronic devices.

Key words wrinkling, finite substrate thickness, theoretical mechanics model

Chinese Library Classification O343.3
2010 Mathematics Subject Classification 74A45, 74A50

1 Introduction

Surface wrinkling is a common phenomenon in daily life. Wrinkling instability is usually considered to be problematic in most applications. However, in some cases, wrinkling can be used to form unique and useful features in optics, electronics mechanics, etc. The wrinkling patterns with such features can be used to enable important applications in many fields such as material metrology and chemosynthesis[1–5].

One method to get the beneficial wrinkling patterns with periodical features is using thin-film-on-elastomer system. A stiff thin film bonded to the surface of a soft substrate, e.g., polydimethylsiloxane (PDMS), can buckle to form periodic wrinkling patterns when the substrate is compressed[6]. Many methods are used to form such wrinkling patterns. Many studies have taken the advantage of the surface oxidation of PDMS by exposing it to UV-ozone or oxygen plasma. These processes create a stiff silica-like material on the surface of the PDMS to form thin-film-on-elastomer system[7–11]. Another robust and controlled process is to fabricate thin-film structures, and then transfer and print them onto the surface of a pre-strained

* Received Sept. 21, 2016 / Revised Nov. 4, 2016
Project supported by the National Natural Science Foundation of China (Nos.11572022 and 11172022)
† Corresponding author, E-mail: mxh@buaa.edu.cn

PDMS substrate[12–14]. The pre-strain relaxation can compress the thin-film to form wrinkling patterns.

One important application of wrinkling patterns is stretchable electronic devices. The wrinkling of thin monocrystalline silicon thin films on elastomers allows the system to be as flexible as soft tissues[15]. Then, it can be reversibly stretched and compressed to large strain without damage. Khang et al.[16] and Jiang et al.[17] produced, for the first time, such systems with PDMS as the substrates.

A few important mechanics models have been developed to study buckling patterns. A model based on a linear perturbation theory is firstly established to determine the critical membrane force causing buckling and the wavelength of wrinkles. In these studies, the wave amplitudes are not determined[18–19]. A few other theoretical models are then introduced to further analyze such problems[20]. Based on the one-dimension (thin-film ribbons or uniaxial loadings on a thin-film plate) model with sinusoidal wrinkles, Chen and Hutchinson[21] obtained the wavelength analytically, and found out that, for two-dimension situations (thin-film plate under biaxial loadings), there were several forms of wrinkles such as labyrinths (disordered zigzag wrinkles), checkerboard, and herringbone modes. They proved that the herringbone mode had the minimum energy among all buckling modes. Song et al.[22] established an analytical approach to study the checkerboard and herringbone buckling modes, obtained the wave length and amplitude of the wrinkling pattern, and proved that the herringbone mode had the lowest energy. There are also studies focusing on other aspects of wrinkling system, e.g., the effects of the materials of the film and substrate and the wrinkle evolution on viscoelastic substrates[23–25].

From the theoretical analysis for relatively small compression (or pre-strain), the wavelength and amplitude of the wrinkling pattern are obtained as follows:

$$A = t_{\mathrm{f}}\sqrt{\frac{\varepsilon_{\mathrm{pre}}}{\varepsilon_{x_{\mathrm{c}}}} - 1}, \tag{1}$$

$$\lambda_{\mathrm{f}} = \frac{\pi t_{\mathrm{f}}}{\sqrt{\varepsilon_{x_{\mathrm{c}}}}}, \tag{2}$$

$$\varepsilon_{x_{\mathrm{c}}} = \frac{1}{4}\Big(\frac{3(1-\nu_{\mathrm{f}}^2)E_{\mathrm{s}}}{(1-\nu_{\mathrm{s}}^2)E_{\mathrm{f}}}\Big)^{\frac{2}{3}}, \tag{3}$$

where A is the amplitude of the wrinkling patterns, and λ_{f} is the wavelength. E_{f} and E_{s} are Young's moduli of the film and the substrate, respectively, and ν_{f} and ν_{s} are Poisson's ratios of the film and the substrate, respectively. t_{f} is the thickness of the film. $\varepsilon_{\mathrm{pre}}$ is the pre-strain applied to the system, and $\varepsilon_{x_{\mathrm{c}}}$ is the critical strain. It is noteworthy that the buckling wave length only varies with the material properties (Young's moduli and Poisson's ratios of the film and the substrate) and the film thickness. The amplitude is related to the material properties, the film thickness, and the pre-strain of the system. When the pre-strain increases, the wavelength remains constant, while the amplitude changes accordingly.

In most theoretical models, the film is regarded as a plate, and the substrate is usually simplified to be a semi-infinite elastomer[26–27], because the thickness of the substrate (centimeters) is 3–5 orders of magnitude larger than that of the film (sub-microns). Huang et al.[26] established an analytical model for finite substrate thickness when the bottom of the substrate is bonded to a rigid support, and obtained an analytical solution for the wavelength and amplitude of the wrinkles.

In the important applications of wrinkling patterns such as stretchable electronic devices, the film-on-elastomer system is usually integrated with the biological tissues such as human brain, skin, and heart. Under such conditions, the thickness of the products should be very small, e.g., $< 100\,\mu$m. In these cases, the substrate can no longer be treated as semi-infinite.

Therefore, a model is established to describe the wrinkling system with a substrate of finite thickness. In this model, the bottom surface of the system is free (see Fig. 1).

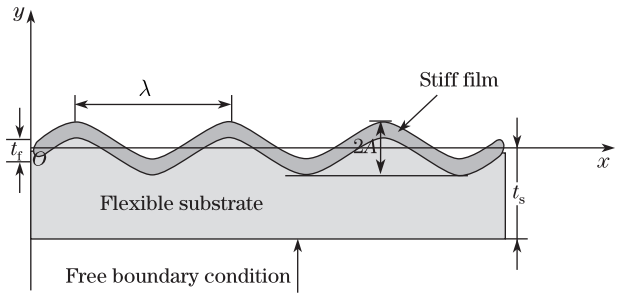

Fig. 1 Schematics of analytical model

2 Analytical model

A Cartesian coordinate system is established with the x-axis on the interface between the film and the substrate and the y-axis along the thickness direction (see Fig. 1). The thicknesses of the film and the substrate are denoted as t_f and t_s, respectively, and $N = t_\mathrm{s}/t_\mathrm{f}$ is the thickness ratio.

The displacements in the substrate are expressed by the variable separation method as follows:

$$u_\mathrm{s}(x,y) = \overline{u}(x)f(y), \tag{4}$$

$$v_\mathrm{s}(x,y) = \overline{v}(x)f(y), \tag{5}$$

where $\overline{u}(x)$ and $\overline{v}(x)$ are determined by known boundary conditions, and $f(y)$ is the decay function which will be solved.

The strains in the substrate can be obtained as follows:

$$\varepsilon_{x_\mathrm{s}} = \frac{\partial u_\mathrm{s}}{\partial x}, \tag{6}$$

$$\varepsilon_{y_\mathrm{s}} = \frac{\partial v_\mathrm{s}}{\partial y}, \tag{7}$$

$$\gamma_{xy_\mathrm{s}} = \frac{\partial u_\mathrm{s}}{\partial y} + \frac{\partial v_\mathrm{s}}{\partial x}, \tag{8}$$

$$\varepsilon_{x_\mathrm{s}} = \overline{u}'(x)f(y), \tag{9}$$

$$\varepsilon_{y_\mathrm{s}} = \overline{v}(x)f'(y), \tag{10}$$

$$\gamma_{xy_\mathrm{s}} = \overline{u}(x)f'(y) + \overline{v}'(x)f(y). \tag{11}$$

The normal and shear stresses can be obtained as follows:

$$\sigma_{x_\mathrm{s}} = E_{\mathrm{s}1}\varepsilon_{x_\mathrm{s}} + E_{s2}\varepsilon_{y_\mathrm{s}}, \tag{12}$$

$$\sigma_{y_\mathrm{s}} = E_{\mathrm{s}2}\varepsilon_{x_\mathrm{s}} + E_{s1}\varepsilon_{y_\mathrm{s}}, \tag{13}$$

$$\tau_{xy_\mathrm{s}} = G_\mathrm{s}\gamma_{xy_\mathrm{s}}. \tag{14}$$

For the plane strain case, we have

$$E_{\mathrm{s}1}=\frac{E_{\mathrm{s}}}{1-\nu^2}, \tag{15}$$

$$E_{\mathrm{s}2}=\frac{E_{\mathrm{s}}\nu}{1-\nu^2}, \tag{16}$$

$$G_{\mathrm{s}}=\frac{E_{\mathrm{s}}}{2(1+\nu)}, \tag{17}$$

where E_{s}, ν, and G_{s} are Young's modulus, Poisson's ratio, and the shear modulus of the substrate, respectively.

The variation principle for the substrate is expressed as follows:

$$\int_{-t_{\mathrm{s}}}^{0}\int_{0}^{l}\Big(\frac{\partial\sigma_{x_{\mathrm{s}}}}{\partial x}+\frac{\partial\tau_{xy_{\mathrm{s}}}}{\partial y}\Big)\delta u_{\mathrm{s}}\mathrm{d}x\mathrm{d}y+\int_{-t_{\mathrm{s}}}^{0}\int_{0}^{l}\Big(\frac{\partial\sigma_{y_{\mathrm{s}}}}{\partial y}+\frac{\partial\tau_{xy_{\mathrm{s}}}}{\partial x}\Big)\delta v_{\mathrm{s}}\mathrm{d}x\mathrm{d}y=0, \tag{18}$$

where

$$\delta u_{\mathrm{s}}=\overline{u}(x)\delta f(y), \tag{19}$$

$$\delta v_{\mathrm{s}}=\overline{v}(x)\delta f(y), \tag{20}$$

and l is the length. When only one wavelength is considered, $l=\lambda_{\mathrm{f}}$.

Substituting Eqs. (4) and (5) into Eq. (18), we get

$$\int_{-t_{\mathrm{s}}}^{0}\int_{0}^{l}\Big(\Big(\frac{\partial\sigma_{x_{\mathrm{s}}}}{\partial x}+\frac{\partial\tau_{xy_{\mathrm{s}}}}{\partial y}\Big)\overline{u}(x)+\Big(\frac{\partial\sigma_{y_{\mathrm{s}}}}{\partial y}+\frac{\partial\tau_{xy_{\mathrm{s}}}}{\partial x}\Big)\overline{v}(x)\Big)\mathrm{d}x\mathrm{d}y=0. \tag{21}$$

From Eqs. (6)–(14) and (21), we can obtain a second-order homogeneous differential equation as follows:

$$af''(y)+bf'(y)+cf(y)=0, \tag{22}$$

where

$$a=G_{\mathrm{s}}\int_{0}^{l}\overline{u}^2(x)\mathrm{d}x+E_{\mathrm{s}1}\int_{0}^{l}\overline{v}^2(x)\mathrm{d}x, \tag{23}$$

$$\begin{aligned}b&=(E_{\mathrm{s}2}+G_{\mathrm{s}})\int_{0}^{l}\overline{v}'(x)\overline{u}(x)\mathrm{d}x+(E_{\mathrm{s}2}+G_{\mathrm{s}})\int_{0}^{l}\overline{u}'(x)\overline{v}(x)\mathrm{d}x\\&=(E_{\mathrm{s}2}+G_{\mathrm{s}})\int_{0}^{l}(\overline{u}(x)\overline{v}(x))'\mathrm{d}x\\&=(E_{\mathrm{s}2}+G_{\mathrm{s}})(\overline{u}(l)\overline{v}(l)-\overline{u}(0)\overline{v}(0)),\end{aligned} \tag{24}$$

$$c=E_{\mathrm{s}1}\int_{0}^{l}\overline{u}''(x)\overline{u}(x)\mathrm{d}x+G_{\mathrm{s}}\int_{0}^{l}\overline{v}''(x)\overline{v}(x)\mathrm{d}x. \tag{25}$$

The eigenvalue of Eq. (22) can be determined by

$$a\lambda^2+b\lambda+c=0. \tag{26}$$

Thus, $f(y)$ can be expressed by

$$f(y) = \alpha_1 \mathrm{e}^{\lambda_1 y} + \alpha_2 \mathrm{e}^{\lambda_2 y}, \tag{27}$$

where

$$\lambda_{1,2} = \frac{-b \pm \sqrt{b^2 - 4ac}}{2a}. \tag{28}$$

At the interface between the film and the substrate $y = 0$, based on the continuity condition, we have

$$f(0) = 1. \tag{29}$$

Thus, we get

$$\alpha_1 + \alpha_2 = 1, \tag{30}$$

$$f(y) = \alpha_1 \mathrm{e}^{\lambda_1 y} + (1 - \alpha_1)\mathrm{e}^{\lambda_2 y}. \tag{31}$$

The other three edges are free. Therefore, we can write the corresponding boundary condition as follows:

$$\int_{C_\mathrm{f}} ((\sigma_{x_\mathrm{s}} \cos\theta + \tau_{xy_\mathrm{s}} \sin\theta)\delta u_\mathrm{s} + (\tau_{xy_\mathrm{s}} \cos\theta + \sigma_{x_\mathrm{s}} \sin\theta)\delta v_\mathrm{s})\mathrm{d}S = 0, \tag{32}$$

where C_f means the integration path along the side edges and the bottom. Transforming Eq. (32) to the boundary conditions along the side edges and bottom, we get

$$-\int_{-t_\mathrm{s}}^{0} \sigma_{x_\mathrm{s}} \overline{u}(0)\delta f(y)\mathrm{d}y + \int_0^l \sigma_{y_\mathrm{s}} \overline{v}(x)\delta f'(-t_\mathrm{s})\mathrm{d}x + \int_{-t_\mathrm{s}}^{0} \sigma_{x_\mathrm{s}} \overline{u}(l)\delta f(y)\mathrm{d}y = 0. \tag{33}$$

From Eq. (31), we have

$$\delta f(y) = (\mathrm{e}^{\lambda_1 y} - \mathrm{e}^{\lambda_2 y})\delta\alpha_1. \tag{34}$$

From Eqs. (33) and (34), we get

$$m\alpha_1 + n = 0,$$

where

$$\begin{aligned} m = & -E_{\mathrm{s}1}\overline{u}'(0)\overline{u}(0)\int_{-t_\mathrm{s}}^{0}(\mathrm{e}^{\lambda_1 y} - \mathrm{e}^{\lambda_2 y})^2\mathrm{d}y \\ & - E_{\mathrm{s}2}\overline{u}(0)\overline{v}(0)\int_{-t_\mathrm{s}}^{0}(\lambda_1\mathrm{e}^{\lambda_1 y} - \lambda_2\mathrm{e}^{\lambda_2 y})(\mathrm{e}^{\lambda_1 y} - \mathrm{e}^{\lambda_2 y})\mathrm{d}y \\ & + E_{\mathrm{s}2}(\mathrm{e}^{-\lambda_1 t_\mathrm{s}} - \mathrm{e}^{-\lambda_2 t_\mathrm{s}})(\lambda_1\mathrm{e}^{-\lambda_1 t_\mathrm{s}} - \lambda_2\mathrm{e}^{-\lambda_2 t_\mathrm{s}})\int_0^l \overline{u}'(x)\overline{v}(x)\mathrm{d}x \\ & + E_{\mathrm{s}1}(\lambda_1\mathrm{e}^{-\lambda_1 t_\mathrm{s}} - \lambda_2\mathrm{e}^{-\lambda_2 t_\mathrm{s}})^2\int_0^l \overline{v}^2(x)\mathrm{d}x \\ & + E_{\mathrm{s}1}\overline{u}'(l)\overline{u}(l)\int_{-t_\mathrm{s}}^{0}(\mathrm{e}^{\lambda_1 y} - \mathrm{e}^{\lambda_2 y})^2\mathrm{d}y \\ & + E_{\mathrm{s}2}\overline{u}(l)\overline{v}(l)\int_{-t_\mathrm{s}}^{0}(\lambda_1\mathrm{e}^{\lambda_1 y} - \lambda_2\mathrm{e}^{\lambda_2 y})(\mathrm{e}^{\lambda_1 y} - \mathrm{e}^{\lambda_2 y})\mathrm{d}y, \end{aligned}$$

$$
\begin{aligned}
n = & - E_{\mathrm{s}1}\overline{u}'(0)\overline{u}(0)\int_{-t_{\mathrm{s}}}^{0}\mathrm{e}^{\lambda_2 y}(\mathrm{e}^{\lambda_1 y}-\mathrm{e}^{\lambda_2 y})\mathrm{d}y \\
& - E_{\mathrm{s}2}\overline{u}(0)\overline{v}(0)\int_{-t_{\mathrm{s}}}^{0}\lambda_2\mathrm{e}^{\lambda_2 y}(\mathrm{e}^{\lambda_1 y}-\mathrm{e}^{\lambda_2 y})\mathrm{d}y \\
& + E_{\mathrm{s}2}\mathrm{e}^{-\lambda_2 t_{\mathrm{s}}}(\lambda_1\mathrm{e}^{-\lambda_1 t_{\mathrm{s}}}-\lambda_2\mathrm{e}^{-\lambda_2 t_{\mathrm{s}}})\int_{0}^{l}\overline{u}'(x)\overline{v}(x)\mathrm{d}x \\
& + E_{\mathrm{s}1}(\lambda_2\mathrm{e}^{-\lambda_2 t_{\mathrm{s}}})(\lambda_1\mathrm{e}^{-\lambda_1 t_{\mathrm{s}}}-\lambda_2\mathrm{e}^{-\lambda_2 t_{\mathrm{s}}})\int_{0}^{l}\overline{v}^2(x)\mathrm{d}x \\
& + E_{\mathrm{s}1}\overline{u}'(l)\overline{u}(l)\int_{-t_{\mathrm{s}}}^{0}\mathrm{e}^{\lambda_2 y}(\mathrm{e}^{\lambda_1 y}-\mathrm{e}^{\lambda_2 y})\mathrm{d}y \\
& + E_{\mathrm{s}2}\overline{u}(l)\overline{v}(l)\int_{-t_{\mathrm{s}}}^{0}(\lambda_2\mathrm{e}^{\lambda_2 y})(\mathrm{e}^{\lambda_1 y}-\mathrm{e}^{\lambda_2 y})\mathrm{d}y.
\end{aligned}
$$

Thus, $f(y)$ can be determined if the material properties and wrinkling form of the wrinkling system are given.

The strain energy of the substrate is

$$
U_{\mathrm{s}} = \frac{1}{2}\int\int(\sigma_{x_{\mathrm{s}}}\varepsilon_{x_{\mathrm{s}}}+\sigma_{y_{\mathrm{s}}}\varepsilon_{y_{\mathrm{s}}}+\tau_{xy_{\mathrm{s}}}\gamma_{xy_{\mathrm{s}}})\mathrm{d}x\mathrm{d}y. \tag{35}
$$

The strain energy per unit length is

$$
U_{\mathrm{s}} = \frac{1}{2\lambda_{\mathrm{f}}}\int_{0}^{\lambda_{\mathrm{f}}}\int_{-t_{\mathrm{s}}}^{0}(\sigma_{x_{\mathrm{s}}}\varepsilon_{x_{\mathrm{s}}}+\sigma_{y_{\mathrm{s}}}\varepsilon_{y_{\mathrm{s}}}+\tau_{xy_{\mathrm{s}}}\gamma_{xy_{\mathrm{s}}})\mathrm{d}x\mathrm{d}y. \tag{36}
$$

All the terms in Eq. (36) can be determined once the material properties and wrinkling pattern parameters are given. Thus, the strain energy of the substrate can be determined.

The strain energy of the thin film consists of two parts, i.e., the membrane energy and the bending energy.

According to the continuity of the displacement at the interface, the displacements of the film are just the same with those at the top of the substrate, which are $\overline{u}(x)$ and $\overline{v}(x)$.

For a wrinkling pattern system with sinusoidal wrinkles, the specific form of $\overline{v}(x)$ can be easily obtained as follows:

$$
\overline{v}(x) = A\sin(kx), \tag{37}
$$

where A is the amplitude of the wrinkling pattern, and its wavelength λ_{f} is

$$
\lambda_{\mathrm{f}} = \frac{2\pi}{k}. \tag{38}
$$

The bending energy of the film is

$$
U_{\mathrm{b}} = \frac{\overline{E}_{\mathrm{f}}t_{\mathrm{f}}^3}{24\lambda_{\mathrm{f}}}\int_{0}^{\lambda_{\mathrm{f}}}\Big(\frac{\mathrm{d}^2\overline{v}(x)}{\mathrm{d}x^2}\Big)^2\mathrm{d}x = -\frac{A^2\pi^4\overline{E}_{\mathrm{f}}}{3{\lambda_f}^4}(t_{\mathrm{f}})^3, \tag{39}
$$

where

$$
\overline{E}_{\mathrm{f}} = \frac{E_{\mathrm{f}}}{1-\nu_{\mathrm{f}}^2}. \tag{40}
$$

To obtain the membrane energy of the film, the membrane strain $\varepsilon_{\mathrm{mem}}$ must be determined. The membrane strain can be solved from a model of the elastic von Karman plate[29] by

$$\varepsilon_{\mathrm{mem}} = \frac{A^2\pi^2}{A_{\mathrm{f}}^2} - \varepsilon_{\mathrm{pre}}, \tag{41}$$

which is constant along the x-axis.

Then, $\overline{u}(x)$ can also be determined by

$$\overline{u}(x) = \varepsilon_{\mathrm{mem}} x. \tag{42}$$

The membrane energy can be obtained by

$$U_{\mathrm{m}} = \frac{\overline{E}_{\mathrm{f}}}{2\lambda_{\mathrm{f}}} \int_0^{\lambda_{\mathrm{f}}} (\varepsilon_{\mathrm{mem}})^2 \mathrm{d}x = \frac{t_{\mathrm{f}}}{2} \overline{E}_{\mathrm{f}} \Big(\frac{A^2\pi^2}{\lambda_{\mathrm{f}}^2} - \varepsilon_{\mathrm{pre}} \Big)^2. \tag{43}$$

The total energy of the system is

$$U_{\mathrm{tot}} = U_{\mathrm{m}} + U_{\mathrm{b}} + U_{\mathrm{s}}. \tag{44}$$

The wrinkling configuration can be obtained by minimizing the total energy with respect to the amplitude and wave length, i.e.,

$$\frac{\partial U_{\mathrm{tot}}}{\partial A} = 0, \quad \frac{\partial U_{\mathrm{tot}}}{\partial \lambda_{\mathrm{f}}} = 0. \tag{45}$$

3 Results and discussion

The numerical method is used to find the wrinkling configuration under certain conditions.

The material properties in the study are as follows. For the substrate, Young's modulus E_{s} is 2 MPa, and Poisson's ratio ν_{s} is 0.48. For the film, Young's modulus E_{f} is 130 GPa, and Poisson's ratio ν_{f} is 0.27.

As previously described, the key point in this study is the free boundary condition and the finite substrate thickness. Figure 2 shows the function $f(y)$ for different thickness ratios N. The vertical axis in Fig. 2 denotes the value of $f(y)$, and the horizontal axis denotes the y-position percentage with zero for the top surface of the substrate and 100% for the free bottom surface. Figure 2 shows that, when N is relativity small, e.g., $N = 50$, $f(y)$ does not reach zero even at the bottom of the substrate. This indicates that, for small N, the behavior of the wrinkling system apparently differs from the systems within finite substrate thickness. When N is larger than 200, the value of $f(y)$ at the bottom surface is very close to zero (less than 5% error). When N increases to 500, the displacement at the bottom surface decays to almost zero, which is similar to the case of infinite substrate thickness.

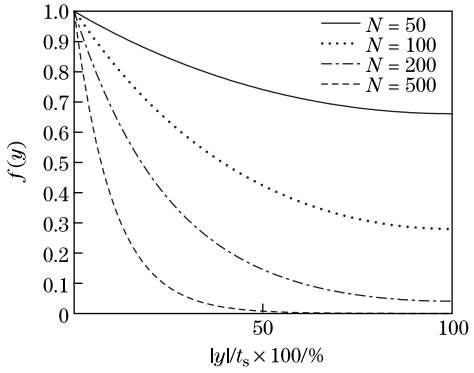

Fig. 2 Decay function $f(y)$ in thickness direction for various values of N

The following study is concentrated on the cases of $N < 500$. Three kinds of film thickness, i.e., 150 nm, 200 nm, and 250 nm, are studied in this paper. With the infinite thickness substrate model in Ref. [21], the amplitude and wavelength in the wrinkling system can be obtained from Eqs. (1)–(3). For the given material properties, the wrinkling parameter can be obtained as follows: $A = 0.974\,\mu\text{m}$, and $\lambda_f = 32.9\,\mu\text{m}$.

Figures 3 and 4 show the variations of the buckling amplitude and wavelength versus the thickness ratio N. It is obvious that when the thickness ratio is relatively small, the results in this study differ greatly from the results for infinite substrate thickness[21] (20% to 30% difference). Both the amplitude and wavelength for finite substrate thickness are larger than those obtained by the infinite thickness model, especially when $N < 200$. Therefore, the assumption of semi-infinite elastomer substrate is not valid anymore when $N < 200$. The results converge quickly to that with infinite thickness substrate when $N > 200$. When $N > 200$, the decay function (or the displacements) decays to almost zero at the bottom surface, and is approximately the same as the infinite boundary condition.

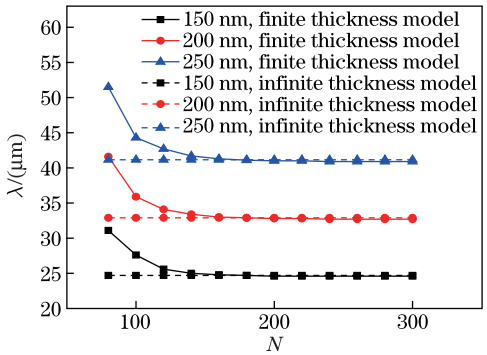

Fig. 3 Variations of wavelength versus thickness ratio N

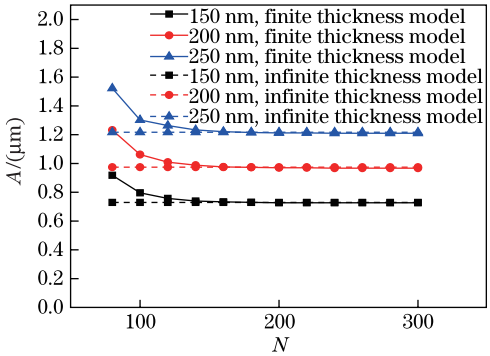

Fig. 4 Variations of amplitude versus thickness ratio N

A calculation is made with the same material parameters with the previous model. Figures 5 and 6 show the variations of the amplitude and wavelength versus various levels of pre-strain when $N = 500$. From the figures, we can see that, when $N = 500$ or the substrate thickness is very large, the results obtained based on the model in this study agree very well with those obtained based on the previous infinite thickness model[21], which verify the validity of this new model. The amplitude is proportional to the pre-strain, while the wavelength remains constant for various levels of pre-strain, which are consistent with the expressions in Eqs. (43) and (44).

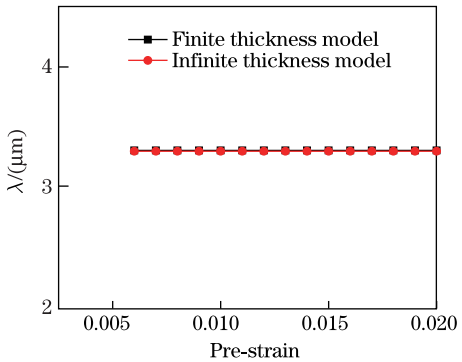

Fig. 5 Variations of wavelength versus pre-strain

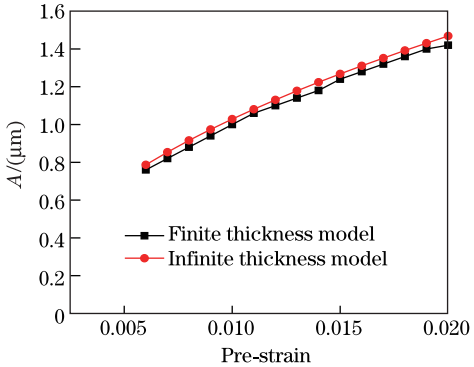

Fig. 6 Variations of amplitude versus pre-strain

The variations of the amplitude and wavelength with different pre-strain are discussed below when the thickness ratio is very small, e.g., $N = 50$. Figures 7 and 8 show that the tendency does not change when the thickness ratio decreases, indicating that the wavelength of the wrinkling pattern depends only on the material properties of the film and the substrate. When larger pre-strain is applied on the system, the wavelength of the wrinkling pattern remains constant, while the amplitude increases.

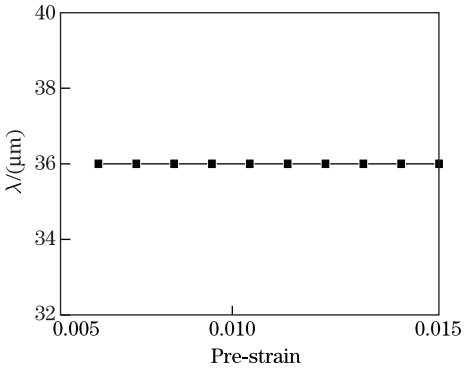

Fig. 7 Variations of wavelength versus pre-strain when $N = 50$

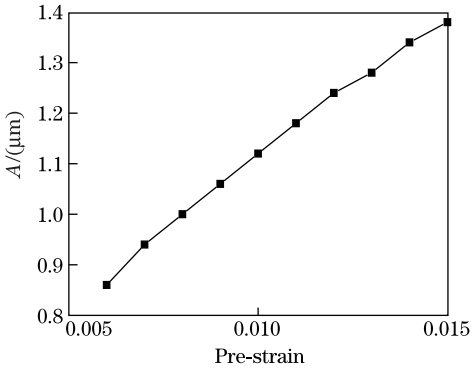

Fig. 8 Variations of amplitude versus pre-strain when $N = 50$

4 Concluding remarks

An analytical model for the wrinkling of thin-film-on-elastomer system with finite substrate thickness is established. The wave length and amplitude of the wrinkling pattern are determined analytically. The results indicate that, when the thickness ratio is less than 200, the effect of finite substrate thickness becomes significant, and both the amplitude and wavelength are much larger than those obtained from infinite thickness models. Similar to the case of infinite substrate thickness, the wavelength is independent of the pre-strain even when the substrate thickness is very small.

References

[1] Schweikart, A., Horn, A., Böker, A., and Fery, A. Controlled wrinkling as a novel method for the fabrication of patterned surfaces. *Complex Macromolecular Systems* I, Springer, Heidelberg (2009)

[2] Nolte, A. J., Rubner, M. F., and Cohen, R. E. Determining the Young's modulus of polyelectrolyte multilayer films via stress-induced mechanical buckling instabilities. *Macromolecules*, **38**, 5367–5370 (2005)

[3] Chung, J. Y., Nolte, A., and Stafford, C. M. Surface wrinkling: a versatile platform for measuring thin-film properties. *Advanced Materials*, **23**, 349–368 (2011)

[4] Bechert, D. W., Bruse, M., Hage, W., and Meyer, R. Fluid mechanics of biological surfaces and their technological application. *Naturwissenschaften*, **87**, 157–171 (2000)

[5] Fürstner, R., Barthlott, W., Neinhuis, C., and Walzel, P. Wetting and self-cleaning properties of artificial superhydrophobic surfaces. *Langmuir*, **21**, 956–961 (2005)

[6] Bowden, N., Brittain, S., Evans, A. G., Hutchinson, J. W., and Whitesides, G. M. Spontaneous formation of ordered structures in thin films of metals supported on an elastomeric polymer. *nature*, **393**, 146–149 (1998)

[7] Chua, D. B., Ng, H. T., and Li, S. F. Spontaneous formation of complex and ordered structures on oxygen-plasma-treated elastomeric polydimethylsiloxane. *Applied Physics Letters*, **76**, 721–723 (2000)

[8] Efimenko, K., Wallace, W. E., and Genzer, J. Surface modification of Sylgard-184 poly (dimethyl siloxane) networks by ultraviolet and ultraviolet/ozone treatment. *Journal of Colloid and Interface Science*, **254**, 306–315 (2002)

[9] Ouyang, M., Yuan, C., Muisener, R. J., Boulares, A., and Koberstein, J. T. Conversion of some siloxane polymers to silicon oxide by UV/ozone photochemical processes. *Chemistry of Materials*, **12**, 1591–1596 (2000)

[10] Genzer, J. and Efimenko, K. Creating long-lived superhydrophobic polymer surfaces through mechanically assembled monolayers. *Science*, **290**, 2130–2133 (2000)

[11] Efimenko, K., Rackaitis, M., Manias, E., Vaziri, A., Mahadevan, L., and Genzer, J. Nested self-similar wrinkling patterns in skins. *Nature Materials*, **4**, 293–297 (2005)

[12] Sun, Y., Choi, W. M., Jiang, H., Huang, Y. Y., and Rogers, J. A. Controlled buckling of semiconductor nanoribbons for stretchable electronics. *Nature Nanotechnology*, **1**, 201–207 (2006)

[13] Loo, Y. L., Hsu, J. W., Willett, R. L., Baldwin, K. W., West, K. W., and Rogers, J. A. High-resolution transfer printing on GaAs surfaces using alkane dithiol monolayers. *Journal of Vacuum Science and Technology B*, **20**, 2853–2856 (2002)

[14] Zhang, H. L., Okayasu, T., and Bucknall, D. G. Large area ordered lateral patterns in confined polymer thin films. *European Polymer Journal*, **40**, 981–986 (2004)

[15] Song, J., Feng, X., and Huang, Y. Mechanics and thermal management of stretchable inorganic electronics. *National Science Review*, **3**, 128–143 (2016)

[16] Khang, D. Y., Jiang, H., Huang, Y., and Rogers, J. A. A stretchable form of single-crystal silicon for high-performance electronics on rubber substrates. *Science*, **311**, 208–212 (2006)

[17] Jiang, H., Khang, D. Y., Song, J., Sun, Y., Huang, Y., and Rogers, J. A. Finite deformation mechanics in buckled thin films on compliant supports. *Proceedings of the National Academy of Sciences*, **104**, 15607–15612 (2007)

[18] Niu, K. and Talreja, R. Modeling of wrinkling in sandwich panels under compression. *Journal of Engineering Mechanics*, **125**, 875–883 (1999)

[19] Volynskii, A. L., Bazhenov, S., Lebedeva, O. V., and Bakeev, N. F. Mechanical buckling instability of thin coatings deposited on soft polymer substrates. *Journal of Materials Science*, **35**, 547–554 (2000)

[20] Huang, Z., Hong, W., and Suo, Z. Evolution of wrinkles in hard films on soft substrates. *Physical Review E*, **70**, 030601 (2004)

[21] Chen, X. and Hutchinson, J. W. Herringbone buckling patterns of compressed thin films on compliant substrates. *Journal of Applied Mechanics*, **71**, 597–603 (2004)

[22] Song, J., Jiang, H., Choi, W. M., Khang, D. Y., Huang, Y., and Rogers, J. A. An analytical study of two-dimensional buckling of thin films on compliant substrates. *Journal of Applied Physics*, **103**, 014303 (2008)

[23] Chen, Z., Kim, Y. Y., and Krishnaswamy, S. Anisotropic wrinkle formation on shape memory polymer substrates. *Journal of Applied Physics*, **112**, 124319 (2012)

[24] Li, J., An, Y., Huang, R., Jiang, H., and Xie, T. Unique aspects of a shape memory polymer as the substrate for surface wrinkling. *ACS Applied Materials and Interfaces*, **4**, 598–603 (2012)

[25] Huang, Z., Hong, W., and Suo, Z. Evolution of wrinkles in hard films on soft substrates. *Physical Review E*, **70**, 030601 (2004)

[26] Huang, Z. Y., Hong, W., and Suo, Z. Nonlinear analyses of wrinkles in a film bonded to a compliant substrate. *Journal of the Mechanics and Physics of Solids*, **53**, 2101–2118 (2005)

[27] Lin, P. C. and Yang, S. Spontaneous formation of one-dimensional ripples in transit to highly ordered two-dimensional herringbone structures through sequential and unequal biaxial mechanical stretching. *Applied Physics Letters*, **90**, 241903 (2007)

[28] Timoshenko, S. P. and Gere, J. M. *Theory of Elastic Stability*, Dover Publications, New York (2009)

[29] Timoshenko, S. P. and Woinowsky-Krieger, S. *Theory of Plates and Shells*, Mcgraw-Hill College, New York (1959)